A Novel Potential Line Strategy for Autonomous Vehicle Control in Lane-free Traffic

Hanwen Zhang[1], Majid Rostami-Shahrbabaki[1], Dimitrios Troullinos[2], and Klaus Bogenberger[1]

Abstract— **Recent developments in vehicular traffic have brought about the concept of lane-free traffic, challenging the traditional notion of parallel lanes, allowing vehicles to potentially drive at any arbitrary lateral location of the road. In this paper, we investigate the potential lines strategy proposed in our previous study for an efficient lateral distribution of vehicles in automated lane-free freeways. Potential lines allow for structured lane-free traffic where each vehicle receives a desired lateral location based on its desired speed. To this end, we mimic the behavior of conventional driving by assigning the right side of the road to slower vehicles while faster vehicles are led toward the left. As a result, the road surface effectively forms a speed-based hierarchy, with vehicles flowing smoothly from right to left in a monotonic increase of speed. We utilize the Probability Integral Transform approach to have a uniform lateral distribution of potential lines despite different distributions of desired speed. In addition, we show that the potential lines are efficient means of handling different maneuvers such as merge, diverge, and emergency vehicle preemption on a freeway. The simulation results for a relatively long freeway demonstrate that potential lines can minimize unnecessary lateral movement during overtaking, creating a more structured and efficient driving environment. Furthermore, results show that potential lines can smoothly guide vehicles to take off-ramps or merge from on-ramps in high-density traffic conditions.**

I. INTRODUCTION

The 21st century has seen the automotive industry's rapid growth, bringing significant challenges. Increased traffic has sparked worldwide road construction, yet congestion continues to escalate [1]. Additionally, the rapid increase in vehicles and urban road infrastructure contributes to environmental problems and poses serious health risks. This growth is accompanied by an even more alarming consequence: road traffic accidents have emerged as one of the leading causes of death and physical disability worldwide [2].

In pursuit of greater efficiency and safety in transportation, research has focused on Connected and Automated Vehicles (CAVs) [3] and Intelligent Transportation Systems (ITS) [4]. CAVs, a groundbreaking technology, hold the potential to reduce accidents and enhance transportation system performance, while ITS, with Perception and Communication Technology, aims to improve safety and promote sustainable transportation. The real-time Vehicle-to-Everything (V2X) and Vehicle-to-Vehicle (V2V) communication, enable CAVs to constantly sense traffic participants and gather information. The synergy between CAVs and ITS technologies paints a promising picture for the future of transportation.

The concept of parallel lanes was introduced in the last century, aiming to improve traffic safety [5]. However, in the era of CAVs and ITS, the necessity of lanes is being questioned since CAVs are capable of rapidly and continuously monitoring their surroundings and other vehicles reliably, in addition to communicating and making swift decisions [6]. Papageorgiou et al. (2021) pointed out that the implementation of lanes results in a high reduction in the lateral utilization rate of freeways as their lateral occupancy is only slightly higher than 50%, in general [7]. Furthermore, in some developing countries, the phenomenon was observed that low lane discipline contributes to an increase in saturation flow at traffic lights under non-homogeneous traffic conditions. Consequently, they suggested that in the future, the lane structure of freeways, motorways, arterials, and even urban roads could be eliminated, also known as the concept of lane-free traffic (LFT), in which CAVs are no longer constrained by the lateral movement requirements of lanes and can drive along arbitrary lateral locations of the road. This would increase the overall capacity of the road network and avoid land consumption associated with constructing additional roads. In this context, Sekeran et al. (2022) provided a comprehensive overview of the factors influencing research and implementation of LFT, setting the foundation for various studies in this area [8]. In addition, Papageorgiou et al. [7] introduced the concept of nudging in LFT, which refers to the process wherein vehicles adjust their behavior upon detecting faster approaching vehicles from behind. This adjustment typically involves moving diagonally along the interaction line between the two vehicles, creating sufficient space for the trailing vehicle to overtake safely. In a macroscopic view, nudging implies that the traffic flow could also be affected by the upstream traffic conditions.

Since the introduction of the LFT, many researchers have addressed different aspects of vehicle control in this new traffic environment. Levy and Haddad (2021) [9] developed and demonstrate the effectiveness of a nonlinear Model Predictive Controller for trajectory planning and control of fully autonomous vehicles on lane-free roads through case study simulations. In a related effort, Yanumula et al. (2023) [10] presented an optimal control motion planning algorithm for CAVs in lane-free freeways, showcasing promising results in traffic simulation at the network and vehicle level. Subsequently, drawing inspiration from migratory bird flocking, the

*This work is based on the project "Simulation and organization of future lane-free traffic" funded by the German research foundation (DFG), under the project number BO 5959/1-1.

[1]Hanwen Zhang, Majid Rostami-Shahrbabaki, and Klaus Bogenberger are with the Chair of Traffic Engineering and Control, Technical University of Munich, Germany. Corresponding author: majid.rostami@tum.de

[2]Dimitrios Troullinos is with Dynamic Systems and Simulation Laboratory, Technical University of Crete, Chania, Crete, 73100, Greece.

"flocking" concept in LFT is introduced and developed in [11], [12] as the generalization of vehicle platooning. Berahman et al. (2022) [13] introduced a novel driving strategy that utilizes artificial forces and reinforcement learning to ensure safe driving behavior and improve the network throughput of CAVs in LFT. Inspired by an adaptive cruise control scheme, Malekzadeh et al. (2022) [14] introduced a unique vehicle movement strategy for LFT based on repulsive and nudging forces, investigate its impact on traffic flow and safety through simulation, and demonstrate improvements in traffic capacity via vehicle nudging and road widening.

In right-hand traffic (RHT) countries such as European countries and the United States, drivers typically overtake on the left of the vehicle being overtaken, with vehicles on the left usually moving at faster speeds [15]. Drawing inspiration from this, Rostami-Shahrbabaki et al. (2023) proposed the concept of potential lines in LFT [16]. This approach laterally organizes CAVs based on their longitudinal desired speeds, establishing a lane-independent lateral structure and thereby reducing unnecessary lateral movements of CAVs. In this approach, CAVs are allocated different potential lines spanning from left to right, with those desiring higher speeds placed on the left. This encourages CAVs to maintain a trajectory along their designated potential lines. This strategy minimizes lateral speed conflicts and unnecessary lateral maneuvers. In this study, the authors assumed that the desired speeds of CAVs on the road are uniformly distributed, leading to a linear potential line function that, subsequently, creates a uniform distribution of potential lines across the lateral width of the road. Consequently, they conclude that under certain conditions, the potential lines driving strategy can enhance the lateral utilization of the road while maintaining traffic capacity by moderately reducing the road width. However, desired speeds are not always uniformly distributed [17], [18], and the definition of the potential line function should consider the variability of desired speed distributions.

Building upon the previous work, this paper utilizes the Probability Integral Transform concept [19] to optimize the lateral distribution of potential lines, making them applicable to various desired speed distributions for different vehicle types. Using this approach, any distribution of the vehicles' desired speed will be mapped to a uniform lateral distribution of vehicles, leading to an optimized lateral occupancy usage of the road. In addition, We will also introduce how the potential lines can be used to guide vehicles on off-ramps and on-ramps at the motion planning level. This represents an excellent contribution of this work. To the best of the authors' knowledge, this is the first time that lane-free driving strategies have been applied to a freeway network with off-ramps and on-ramps. In this work, we include the merging, diverging, and even weaving phenomenons by simulating a relatively long stretch of freeway which makes the design procedure more complex. Finally, we will demonstrate how the potential line concept can be extended to accomplish emergency vehicle preemption. The outcomes indicate that the potential line strategy effectively reduces unnecessary lateral movement during overtaking by maintaining a structured lane-free environment with laminar traffic flow.

II. Methodology

In presenting our methodology, we divide the control algorithm into three overarching sections: A) *Basic Requirement*, encapsulating a variety of essential methodologies for vehicular control in LFT, including vehicle dynamics, boundary, and desired speed feedback controllers, and the concept of artificial forces for collision avoidance. B) *Potential line*, dealing extensively with the Potential Line function and controller, a mechanism designed to enable vehicles to follow a structured lateral distribution in the LFT environment. Importantly, this part will introduce the utilization of the Probability Integral Transform to optimize the distribution of the Potential Line, a key innovation in our methodology. Finally, C) *Potential line application* describes how the concept of the developed potential line can be used in guiding vehicles to merge from and diverge to ramps and yield to emergency vehicles.

A. Basic requirements

1) Vehicle dynamics: We model vehicle dynamics using the double integrator model represented by discrete-time differential equations that are justified to be used in LFT [10]. The state-space equations for vehicle i, with T being the discrete-time step, and $t = kT$ where $k = 0, 1, ...,$ are presented below:

$$x_{1,i}(k+1) = x_{1,i}(k) + Tx_{2,i}(k) + \frac{1}{2}T^2 u_{x,i}(k) \quad (1a)$$

$$x_{2,i}(k+1) = x_{2,i}(k) + Tu_{x,i}(k) \quad (1b)$$

$$x_{3,i}(k+1) = x_{3,i}(k) + Tx_{4,i}(k) + \frac{1}{2}T^2 u_{y,i}(k) \quad (1c)$$

$$x_{4,i}(k+1) = x_{4,i}(k) + Tu_{y,i}(k) \quad (1d)$$

here, $x_{1,i}$, $x_{2,i}$, $x_{3,i}$, and $x_{4,i}$ represent vehicle's longitudinal position, longitudinal speed, lateral position, and lateral speed, respectively, while $u_{x,i}$ and $u_{y,i}$ denote longitudinal and lateral accelerations. The accelerations are determined based on the controllers defined in the following sections.

2) Feedback loops for cruise controller: The longitudinal acceleration of the vehicles is determined based on two important terms, i.e., a cruise controller that allows vehicles to drive close to their desired speed in lane-free environments and inter-vehicle forces which prohibit collisions. To this end, target speed forces are defined based on the longitudinal target speeds as follows:

$$f^{ts}_{x,i}(k) = k^{ts}_x(v^{ts}_{x,i} - x_{2,i}(k)) \quad (2)$$

where k^{ts}_x is the controller gain and the longitudinal target speed $v^{ts}_{x,i}$ defined as:

$$v^{ts}_{x,i} = min\left\{s_{ts} \cdot x_{2,i}(k), v^d_{x,i}\right\} \quad (3)$$

where s_{ts} is a factor that enables a gradual increase in the target speed, catering to a non-aggressive driving style, and $v^d_{x,i}$ is the longitudinal desired speed. The lateral acceleration is defined based on the inter-vehicle forces and the potential line function described in the following sections.

3) Artificial force: To prevent collisions between vehicles, artificial potential fields, and their induced inter-vehicle forces are used. To this end, we define the following function around vehicle j with respect to vehicle i:

$$F = \frac{M}{\left[\left(\frac{x_{1,j}(k)-x_{1,i}(k)}{0.5\cdot d_{x,j}(k)}\right)^{f_1} + \left(\frac{x_{3,j}(k)-x_{3,i}(k)}{0.5\cdot d_{y,j}(k)}\right)^{f_2}\right]^{f_3} + 1} \tag{4}$$

where M, f_1, f_2, f_3 are function parameters and $d_{x,i}(k)$ and $d_{y,i}(k)$ are, respectively, the major and minor axis of the safety ellipse around the vehicle j, defined based on the vehicle's speed and safety time gaps (see [16] for detailed explanation).

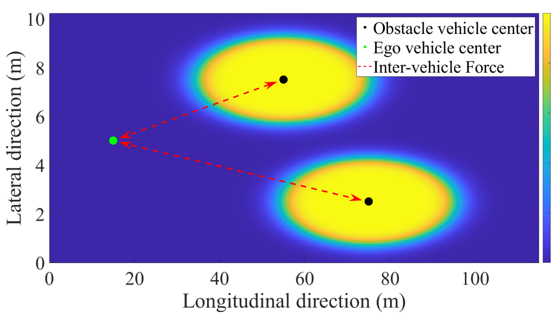

Fig. 1: Artificial potential fields

The potential line function applies inter-vehicle forces between vehicles, guiding the ego vehicle to navigate through areas where the amount of force exerted is minimal, as shown in Figure 1. The force F is projected on the longitudinal and lateral directions creating two forces $f^{pf}_{x,i}$ and $f^{pf}_{y,i}$. The vehicle accelerations are then calculated based on the achieved forces as $u_{x,i}(k) = k^{ts}_x \cdot f^{ts}_{x,i}(k) + k^{pf}_x \cdot f^{pf}_{x,i}(k)$ and $u_{y,i}(k) = k^{pl}_y \cdot f^{pl}_{y,i}(k) + k^{pf}_y \cdot f^{pf}_{y,i}(k)$, where $k^{(.)}_{(.)}$ is a weighting factor and $f^{pl}_{y,i}(k)$ is the potential line force that will be defined in Section II-B.

4) Boundary control and other acceleration constraints: The vehicle accelerations obtained in the previous section are subject to several constraints. More specifically, the lateral movement of the vehicles must be restricted by the road boundaries. This is achieved by employing constraints on lateral acceleration. To this end, we follow the strategy proposed in [14], by first defining two control loops that navigate the vehicle to the left and right boundaries, as shown in Figure 2, for the left road boundary. The necessary accelerations to maintain the boundary control would then be considered as constraints on the lateral accelerations. In addition, both longitudinal and lateral acceleration are bounded by the physical limitation of the vehicle. Overall, the vehicle dynamics are subject to $u_{x,min} \leq u_{x,i}(k) \leq u_{x,max}$ and $u_{y,min}(k) \leq u_{y,i}(k) \leq u_{y,max}(k)$, where the bounds on the longitudinal acceleration are fixed whereas the lateral bounds depends on the boundary control as defined below:

$$u_{y,max}(k) = \min\{U_{y,max},\; k_{P,b}\left[Y_{c,left} - x_{3,i}(k)\right] - k_{D,b} \times x_{4,i}(k)\} \tag{5a}$$

$$u_{y,min}(k) = \max\{U_{y,min},\; k_{P,b}\left[Y_{c,right} - x_{3,i}(k)\right] - k_{D,b} \times x_{4,i}(k)\} \tag{5b}$$

where $k_{P,b}$ and $k_{D,b}$ are controller gains while $Y_{c,left} = Y_{left} - \frac{w_{veh}}{2}$ and $Y_{c,right} = Y_{right} + \frac{w_{veh}}{2}$ are setpints for left and right boundaries control loops, respectively. w_{veh} is the vehicle width as illustrated in Figure 2 and $U_{y,max}$ and $U_{y,max}$ represent fixed lateral limits that restrict the vehicle's movement.

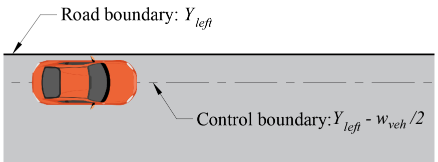

Fig. 2: Left boundary control

This approach ensures that the vehicle's center never crosses the control boundaries, meaning the vehicle's edges will not exceed the road boundaries.

B. Potential line

1) Potential line concept: Theoretically, CAVs can choose arbitrary lateral positions on a lane-free road, leading to complex interactions. These interactions, particularly when involving significant speed disparities, can negatively impact traffic flow, resulting in speed fluctuations, turbulent flows, and increased chaos, especially at higher vehicle densities. Taking cues from common road traffic regulations, where vehicles overtake on the left and slower vehicles occupy the right lanes, Rostami-Shahrbabaki et al. [16] proposed the potential line concept, for reducing unnecessary lateral vehicular movements and achieving structured lateral distribution of CAVs. This distributes vehicles uniformly across the road width based on their desired speeds by assigning them a desired lateral location, fostering a more organized, efficient and laminar traffic flow.

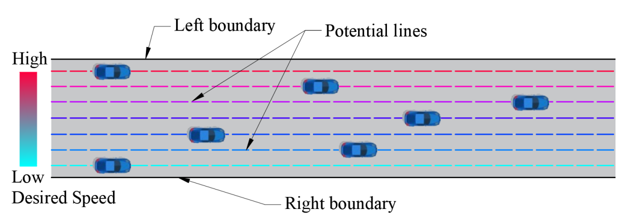

Fig. 3: Potential lines

A freeway segment marked with a series of potential lines is illustrated in Figure 3. It can be observed that across the road width, each CAV on the road is assigned a potential line to drive along; theoretically, infinite number of potential lines may exist. CAVs sharing a common potential line have the same desired speed, with the line at their geometric center. It is worth noting that this example illustrates potential line distribution on a straight freeway section while, in general, the distribution may vary with road shape, motion planning approach, and traffic conditions, as will be explained in Section II-C.

2) Potential line function: In our previous research, we assumed that desired speeds of vehicles follow a uniform distribution. Therefore, we adopted a linear function to map the desired speed distribution to a uniform lateral distribution of vehicles (see [16] for detailed information). In real-world scenarios, the distribution of CAVs' desired speed tends not to be uniform [20]; therefore, a linear mapping leads to an uneven distribution of CAVs on the road when using a linear potential line strategy.

To overcome these limitations, we present a novel approach utilizing the Probability Integral Transform (PIT) in the form of a potential line function. This approach ensures a uniform distribution of vehicles along the lateral axis, irrespective of the underlying distribution of desired speeds. Let us assume a continuous distribution function $f(x)$ for a random variable X, with a cumulative distribution function (CDF) denoted as F_x:

$$F_x(X) = \int_{-\infty}^{X} f(x)dx \tag{6}$$

Then, based on the PIT, a random variable $Y := F_x(X)$ has a standard uniform distribution [19].

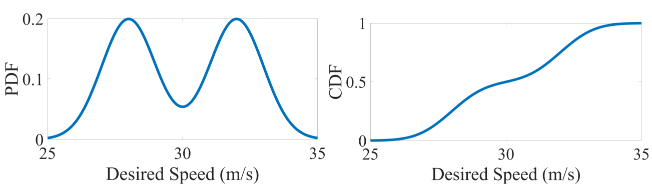

(a) PDF of desired speeds (b) CDF of desired speeds

Fig. 4: Probability Integral Transform

To provide an example, let us consider a scenario where the distribution of vehicles' desired speeds follows a combination of two normal distributions representing fast and slow-moving vehicles, as depicted in Figure 4a, for which the corresponding CDF is illustrated in Figure 4b. According to the PIT theorem, the CDF function maps the desired speed values to a uniform range of $[0, 1]$ uniformly. In the subsequent step, a linear function (7) is employed to map these normalized values to the width of the road, more specifically, in the range of potential line boundaries.

$$y_{pl,i} = Y^{pl}_{right} + (Y^{pl}_{left} - Y^{pl}_{right}) \cdot F(v^d_{x,i}) \tag{7}$$

In essence, this process entails linearly transforming the range of CDF from $[0, 1]$ to $[Y^{pl}_{right}, Y^{pl}_{left}]$. Note that the potential line boundaries may not necessarily be equal to the road boundaries, as will be discussed in Section II-C. Importantly, this approach can be applied to the probability density function of any type that represents the desired speed distributions. By achieving a uniform lateral distribution of CAVs, the method not only ensures efficient utilization of road space but also adapts the potential line function to accommodate various desired speed distributions.

3) Potential line controller: Once the potential line for a vehicle is defined, this value is served as the desired lateral location of the vehicle to drive along. To this end, we use the control law 8 to calculate the corresponding force. Therefore, when the vehicle i deviates from its potential line $y_{pl,i}$, it will be affected by a lateral force $f^{pl}_{y,i}$ towards its potential line.

$$f^{pl}_i(k) = k_{pl}\big(y_{pl,i}(k) - x_{3,i}(k)\big) + k_{pl,v} \cdot x_{4,i}(k) \tag{8}$$

where k_{pl} and $k_{pl,v}$ are the controller gains. As a result, the lateral positioning of CAVs on the road width ensures sufficient separation from vehicles with significantly different desired speeds. Additionally, CAVs operating under potential forces tend to prioritize overtaking from the left side while yielding to vehicles on the right. These characteristics promote organized driving behavior in a lane-free environment, resembling the structure observed in traditional lane-based traffic. By reducing the occurrence of chaotic driving behavior among CAVs, this approach enhances overall traffic throughput, as demonstrated in the forthcoming simulation section.

C. Potential line application

The previous discussion outlined the methodology used to assign potential lines in freeway segments without accounting for variant routes. This becomes more complex when considering freeway segments with on- and off-ramps, which necessitate lateral vehicular movements for merge and diverge maneuvers and requires adaption of the potential lines. Consequently, the following sections will introduce several applications on how potential lines enable merge and diverge maneuvers at off-ramp and on-ramps, as well as the establishment of an emergency vehicle preemption approach.

The potential line boundaries are critical variables to consider in its calculation process, varying with different routes. To structure this discussion more logically, we will tackle off-ramp and on-ramp separately.

1) Off-ramp area: In the off-ramp areas of freeways, vehicles can be primarily categorized into two routes: those proceeding straight and those exiting via the off-ramp, as shown in Figure 5. In the following analysis, we discuss the two above-mentioned types of vehicular flows on distinct paths within the off-ramp area, delving into their unique characteristics and implications.

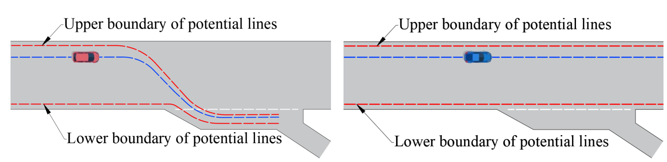

(a) An off-ramp vehicle (b) A straight-through vehicle

Fig. 5: Off-ramp scenario

a) Off-ramp route: CAVs need to a gradual rightward shift to enter the off-ramp approach zone. This is achieved by adjusting the potential line's left boundary and shifting it to the off-ramp approach area. Consequently, the potential lines will be adapted accordingly. As a result, CAVs are continuously and smoothly guided by the corresponding lateral force to drive into the exit zone, as illustrated in Figure 5a.

Off-ramp vehicles, especially faster ones, face speed mismatch issues with CAVs driving on the right side as they traverse to the right. To solve this, we suggest a real-time dynamic adjustment of each vehicle's longitudinal desired speed entering the off-ramp zone. This will enable vehicles to match the lateral desired speeds on the road, facilitating a smoother merging process and avoiding potential conflicts. Therefore, the real-time desired speed of off-ramp vehicles at time step k will be set as:

$$v_{x,i}^{d_{new}}(k) = F^{-1}\left(\frac{x_{3,i}(k-1) - Y_{right}^{pl}}{Y_{left}^{pl} - Y_{right}^{pl}}\right) - v_0 \tag{9}$$

where v_0, is the correction factor for the desired speed, normally considered a constant value between 3 and $5\,m/s$, and F is the CDF function in (6).

In high-density situations, factors such as nudging and repulsive forces of other vehicles may limit the lateral maneuverability of the leaving vehicles at the off-ramp area with the original potential line controller. Therefore, we introduce lateral change willingness by increasing the controller gain k_{pl} (see Equation 8) for the vehicles leaving at off-ramps as:

$$\begin{aligned} k_{pl} = k_{off-ramp_1} \cdot \left(\frac{d}{D} \cdot \frac{x_{3,i}(k)}{R - w_{veh}}\right) \\ + k_{off-ramp_2} \end{aligned} \tag{10}$$

where R is the road width, $k_{off-ramp_1}$ and $k_{off-ramp_2}$ are the controller gains and d indicates the distance of the vehicle from the start of the off-ramp area and D is the approach area length, as depicted in Figure 6.

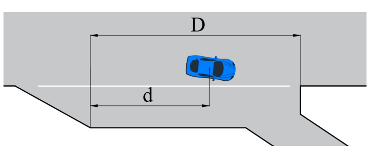

Fig. 6: The vehicle receives more lateral force as it approaches the off-ramp

b) Straight-through route: Since a straight-through vehicle only needs to proceed forward in the off-ramp area, its potential lane boundaries, and therefore the assigned potential line, remain unchanged within this region, as illustrated in Figure 5b.

2) On-ramp area: Similarly, in the on-ramp area, there are also two distinct vehicular flows based on different routes, as depicted in Figure 7. During merging, on-ramp vehicles transition to the freeway, gradually guided by lateral forces provided by their potential lines. A strategy facilitates this process by maintaining boundaries for on-ramp vehicles within the primary freeway zone, as depicted in Figure 7a.

Under conditions of higher demand, a willingness factor similar to that in Equation 10 is introduced to provide enhanced guidance for on-ramp vehicular flows during the merging process. In addition, for straight-through vehicles,

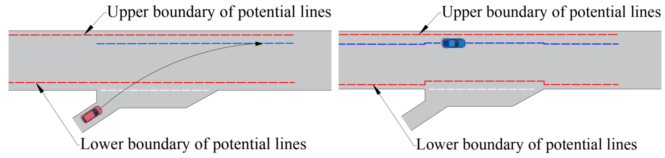

(a) An on-ramp vehicle (b) A straight-through vehicle

Fig. 7: On-ramp scenario

the potential boundaries remain unchanged. However, in situations with high on-ramp demand, it is beneficial to raise the lower boundary of the potential by 1-2 meters, as shown in Figure 7b. This adjustment provides on-ramp vehicles with more lateral space, facilitating a smoother merging process during periods of increased traffic.

3) Emergency vehicle preemption: Another aspect of the potential line application pertains to emergency vehicle preemption, which deals with the prioritization of emergency vehicles. We assume that emergency vehicles always have a higher desired speed compared to regular vehicles. Therefore, according to the potential line strategy, emergency vehicles should always travel as far to the left side of the road as possible.

To enhance the process of yielding to emergency vehicles, we introduce the variable called $\Delta v(k) = x_{2,ev}(k) - v_x^{d_{max}}$, where $x_{2,ev}(k)$ and $v_x^{d_{max}}$ represent the current speed of the emergency vehicle ev and the maximum desired speed of normal CAVs within the road segment, respectively. This variable captures the difference between the emergency vehicle's speed and the maximum desired speed of other vehicles in the vicinity. Based on this definition, we propose the concept of a moving emergency field around the emergency vehicle at time step k. This field extends both in front and behind of the emergency vehicle, with distances calculated as below:

$$\text{if } \Delta \geq 0: \quad \begin{aligned} d_{\text{front}}(k) &= \max\left[d_{\text{long}}, \Delta v(k) \times 60\right] \\ d_{\text{behind}}(k) &= \max\left[d_{\text{short}}, \Delta v(k) \times 10\right] \end{aligned} \tag{11a}$$

$$\text{if } \Delta < 0: \quad \begin{aligned} d_{\text{behind}}(k) &= \max\left[d_{\text{long}}, \Delta v(k) \times 60\right] \\ d_{\text{front}}(k) &= \max\left[d_{\text{short}}, \Delta v(k) \times 10\right] \end{aligned} \tag{11b}$$

where d_{long} and d_{short} are the minimum front and back distances of an emergency field, considered as $300\,m$ and $50\,m$, respectively, throughout the experimental evaluation. To provide a yielding area for emergency vehicles within the so-called emergency field, the upper boundary of the potential line for normal vehicles is shifted downwards by the width of the emergency vehicle plus a safety gap, as illustrated in Figure 8. Note that with the definition for the front and behind distances in equation (11), the emergency field extends more to the front once the emergency vehicle drives faster than other vehicles and spans more the behind as it drives slower.

By employing this approach, normal vehicles can yield to emergency vehicles in a timely manner based on their speed difference. Notably, this consideration is also applicable to situations where emergency vehicles need to come to a full stop in the middle of the road. In this extreme case, upstream vehicles change their lateral location in a prompt manner.

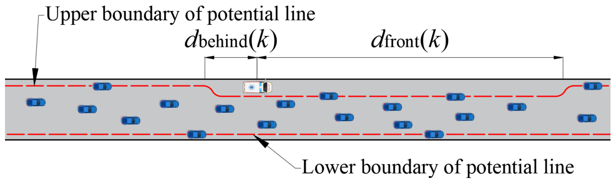

Fig. 8: Emergency field

III. Simulation environment, results and discussion

A. Simulation environment

To evaluate our proposed approach, a freeway network featuring three off-ramps and three on-ramps, as illustrated in Figure 9 is developed. The considered simulation network is a $9\,km$ freeway, with the distance between ramps R1 R2, and R5 R6 being $1\,km$. To intentionally create some bottlenecks, we positioned on-ramp R3 upstream of off-ramp R4 and linked them using a 500-meter-long weaving section where the traffic stream experiences conflicting lateral movements. The network is $10.2\,m$ wide, which corresponds to a 3-lane freeway configuration. Seven detectors are placed at different locations on the freeway, providing necessary traffic state measurements.

For a comprehensive evaluation, a two-hour simulation run with time-varying demand is conducted. Specifically, the demand for straight-through vehicles is adjusted every 800 seconds according to the following sequence [2000, 4000, 6000, 8000, 10000, 12000, 12000, 6000, 2000] veh/h. The demands associated with vehicles exiting from the off-ramps or entering at on-ramps are assumed to have a fixed value of 2000 veh/h. In our simulation scenarios, we accounted for a vehicle's desired speed falling within the interval $[25, 35]\,m/s$. A combination of two groups of fast- and slow-moving vehicles with normal distributions is created, similar to Figure 4a. The mean values are 32 and 28 for the former and latter, respectively, while both have a standard deviation equal to 1.

The simulations were conducted using TrafficFluid-Sim [21], a specialized simulator developed within the SUMO (Simulation of Urban Mobility) microscopic simulator [22] for detailed modeling of CAV interactions in a LFT environment. Utilizing an external application programming interface (API) and a dynamic library to control vehicular dynamics and define driving strategies, particularly in its extended version [23], TrafficFluid-Sim serves as a robust platform for evaluating the effectiveness of CAV strategies within the LFT paradigm.

B. Results and discussion

We will commence our discussion with the results of the lateral distribution of vehicles. Following this, we will analyze the traffic-related results such as speed contour plots, flow-density characteristics, and vehicle trajectories.

To demonstrate the performance of the potential line approach, a dataset consisting of 5,000 vehicles, randomly selected and tracked via the detector positioned at the end of a straight freeway section, i.e., at the location of detector D7, is created. The histograms depicting the distribution of both lateral locations and desired speeds of the recorded vehicles are presented in Figure 10, where each bin on the x-axis corresponds to an interval of 0.1.

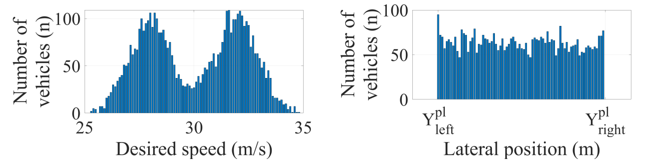

(a) Desired speed distribution (b) Lateral position distribution

Fig. 10: Distributions of the desired speeds and the lateral positions

Figure 10 provides insights into the data distributions, highlighting two key observations. Firstly, the distribution of the desired speeds aligns with the pre-determined normal distributions, as explained earlier. Secondly, as expected, the measured distribution of lateral positions approximates a uniform distribution. Thus, it indicates the fact that the proposed methodology maps the non-uniform desired speed distribution to a uniform distribution of the potential lines. In addition, the potential line controller guides the vehicles along their designated potential line; therefore, maintaining its uniformity.

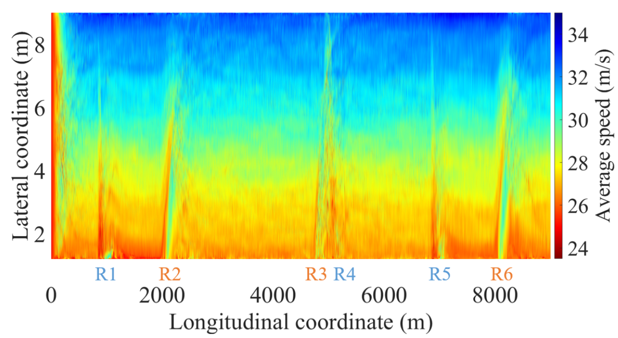

Fig. 11: Speed contour plot for the first hour of simulation

In order to have a better insight of the proposed structured LFT, an average speed contour plot of vehicles for the whole freeway network during the first hour simulation is created and illustrated in Figure 11. A conspicuous trend can be observed that the speed of vehicles gradually increases from the right to the left boundary of the road. This suggests that the potential line strategy influences the way vehicles are distributed laterally over the freeway width, depending on their specific desired speeds. The presence of low-speed values at the beginning of the freeway can be attributed to the frequent lateral changes that occur during this phase. Since vehicles are initially inserted into the network with random lateral locations, it takes some time for them to align themselves with their desired lateral positions. This alignment process involves performing lateral maneuvers, which can temporarily reduce the speed of the vehicles.

Furthermore, the contour plot highlights the presence of shockwaves that occur at the locations of off-ramp and on-ramp maneuvers. Notably, the shockwaves generated at off-ramps propagate in a backward direction. In contrast, the

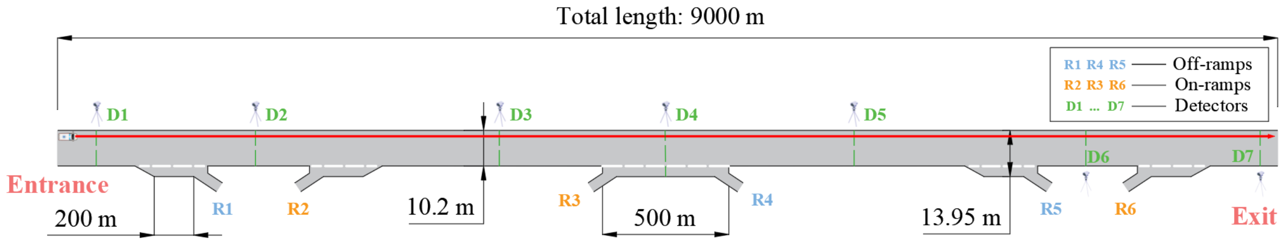

Fig. 9: Freeway scenario

shockwaves observed at on-ramps are forward waves, which is an interesting phenomenon. This can be attributed to the nudging effect caused by vehicles entering the network at on-ramps. The presence of these entering vehicles increases the speed of the vehicles in the mainstream, leading to the formation of forward shockwaves.

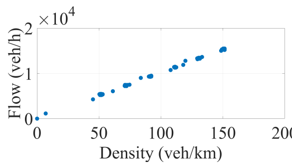

(a) Detector D1

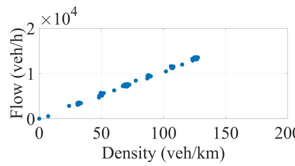

(b) Detector D2

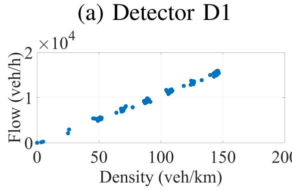

(c) Detector D3

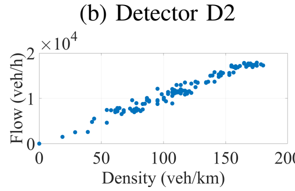

(d) Detector D4

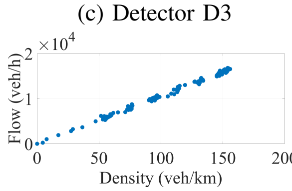

(e) Detector D5

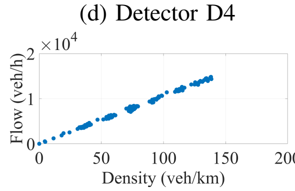

(f) Detector D6

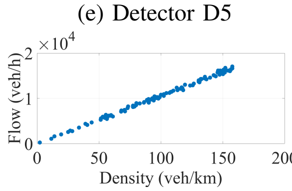

(g) Detector D7

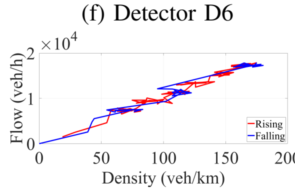

(h) Detector D4 - line graph

Fig. 12: Fundamental diagrams

As mentioned previously, we have strategically placed seven detectors along the freeway to monitor and measure the flow and density of traffic at different sections. The fundamental diagrams, shown in Figure 12, indicate that the overall traffic condition is mostly in a free-flow state. The maximum flow is observed at $13.95\,m$ wide weaving section, as approximately $17,700\,veh/h$, significantly exceeding the typical freeway capacity. This demonstrates the efficiency of the lane-free traffic concept. Dense traffic conditions are primarily observed at the weaving section, i.e., at detector 4, which is expected due to the conflicting lateral movements in this area. However, as shown in Figure 12h with a lower resolution for the fundamental diagram, there is little hysteresis observed. This suggests that there is a minimal capacity drop even in the most challenging section of the road.

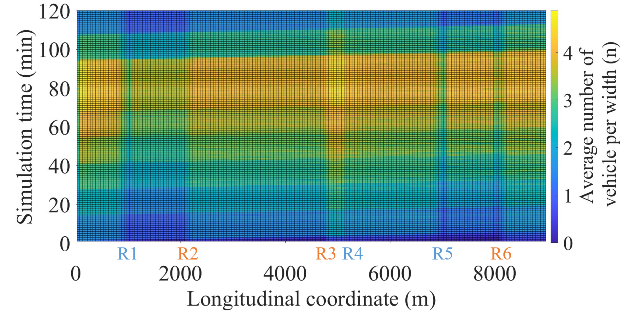

Fig. 13: Average number of vehicles per width over time

Subsequently, the "average number of vehicles per width" using virtual detectors at every $50\,m$ interval is calculated and illustrated in Figure 13. To this end, the presence of a vehicle at one longitudinal location is defined as a Gaussian distribution, whose mean is the longitudinal position of the vehicle's center point, and its standard deviation is set as 0.5 times the vehicle's current speed. Thus, at each measuring point, the expected vehicles per width are calculated by aggregating sum of the vehicle's presence at the detector's location per time-step, averaging these per minute. This definition allows for meaningful measurement of the lateral occupancy of the road. This suggests that during the simulation's high demand period of $53-93\,min$, the network demonstrated superior carrying capacity compared to conventional lane-based traffic.

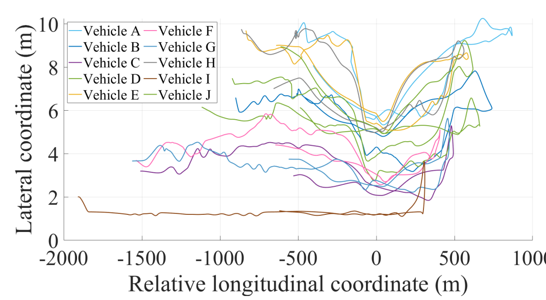

Fig. 14: Trajectories of regular vehicles with respect to the emergency vehicle

Finally, we examine the application of the potential line approach for emergency vehicle (EV) preemption. In this analysis, a speed profile for the emergency vehicle with a desired speed of $40\,m/s$ is assumed, positioning it at the far left side of the road. The EV comes to a full stop in the middle of the road and then accelerates back to its desired speed. We randomly selected 10 vehicles that were originally following the EV. Once the EV comes to a stop, these vehicles overtake it, and then they are overtaken again once the EV speeds up. The relative trajectories of these vehicles with respect to the EV are depicted in Figure 14. It is evident that the vehicle trajectories are guided to the right twice, once when overtaking the EV, and again when the EV overtakes them, demonstrating the effectiveness of the proposed emergency vehicle preemption approach.

Simulation videos, illustrating our proposed approach under various demands in the described freeway network, are available at `https://bit.ly/44pBNaN`.

IV. CONCLUSIONS

For the first time since the introduction of the lane-free traffic concept, this paper presented an investigation into the development of driving strategies for the entire stretch of a freeway, including multiple off-ramps and on-ramps. The key approach employed in this study is the potential line method, which assigns each vehicle a specific desired lateral location to follow. Building upon the principles of probability integral transform, we have further refined the potential line strategy to ensure a uniform lateral distribution of vehicles, irrespective of their desired speed distributions. By implementing this refined potential line strategy, we have successfully promoted structured, lane-free, and laminar traffic flow throughout the freeway, even under high-throughput conditions.

Throughout different applications, the study demonstrated that the potential line strategy serves as an efficient approach for managing various maneuvers on the freeway, including merging, diverging, and preempting for emergency vehicles. Through our analysis, we have demonstrated that the capacity of the freeway can be significantly increased with the implementation of the potential line strategy.

In future studies, we intend to explore and develop additional applications for potential lines beyond the scope of this research. One area of focus will be the development of energy-efficient driving strategies using potential lines. Additionally, we will investigate the utilization of potential lines for managing high-occupancy vehicles on freeways.

REFERENCES

[1] D. Metz, "Tackling urban traffic congestion: The experience of london, stockholm and singapore," *Case Studies on Transport Policy*, vol. 6, no. 4, pp. 494–498, 2018.

[2] A. Mohammed, K. Ambak, A. Mosa, and D. Syamsunur, "A review of the traffic accidents and related practices worldwide," *The Open Transportation Journal*, vol. 13, no. 1, pp. 65–83, 2019.

[3] D. Elliott, W. Keen, and L. Miao, "Recent advances in connected and automated vehicles," *Journal of Traffic and Transportation Engineering (English Edition)*, vol. 6, no. 2, pp. 109–131, 2019.

[4] Y. Lin, P. Wang, and M. Ma, "Intelligent transportation system (its): Concept, challenge and opportunity," in *2017 IEEE 3rd International Conference on Big Data Security on Cloud (BigDataSecurity), IEEE International Conference on High Performance and Smart Computing (HPSC), and IEEE International Conference on Intelligent Data and Security (IDS)*. IEEE, 2017, pp. 167–172.

[5] C. Kun and Y. Lei, "Microscopic traffic-emission simulation and case study for evaluation of traffic control strategies," *Journal of Transportation Systems Engineering and Information Technology*, vol. 7, no. 1, pp. 93–99, 2007.

[6] M. Mushfiq, T. R. Toha, S. I. Salim, A. Mostak, M. Rahaman, N. A. Al-Nabhan, A. M. Sadri, A. Islam *et al.*, "To lane or not to lane? comparing on-road experiences in developing and developed countries using a new simulator" roadbird"," *arXiv preprint arXiv:2010.08590*, 2020.

[7] M. Papageorgiou, K.-S. Mountakis, I. Karafyllis, I. Papamichail, and Y. Wang, "Lane-free artificial-fluid concept for vehicular traffic," *Proceedings of the IEEE*, vol. 109, no. 2, pp. 114–121, 2021.

[8] M. Sekeran, M. Rostami-Shahrbabaki, A. A. Syed, M. Margreiter, and K. Bogenberger, "Lane-free traffic: History and state of the art," in *2022 IEEE 25th International Conference on Intelligent Transportation Systems (ITSC)*, 2022, pp. 1037–1042.

[9] R. Levy and J. Haddad, "Path and trajectory planning for autonomous vehicles on roads without lanes," in *2021 IEEE International Intelligent Transportation Systems Conference (ITSC)*. IEEE, 2021, pp. 3871–3876.

[10] V. K. Yanumula, P. Typaldos, D. Troullinos, M. Malekzadeh, I. Papamichail, and M. Papageorgiou, "Optimal trajectory planning for connected and automated vehicles in lane-free traffic with vehicle nudging," *IEEE Transactions on Intelligent Vehicles*, vol. 8, no. 3, pp. 2385–2399, 2023.

[11] M. Rostami-Shahrbabaki, S. Weikl, M. Akbarzadeh, and K. Bogenberger, "A two-layer approach for vehicular flocking in lane-free environment," in *11th Triennal Symposium on Transportation Analysis (TRISTAN)*, 2022.

[12] M. Rostami-Shahrbabaki, S. Weikl, T. Niels, and K. Bogenberger, "Modeling vehicle flocking in lane-free automated traffic," *Transportation Research Record*, pp. 1–14, 2023.

[13] M. Berahman, M. Rostmai-Shahrbabaki, and K. Bogenberger, "Driving strategy for vehicles in lane-free traffic environment based on deep deterministic policy gradient and artificial forces," *IFAC-PapersOnLine*, vol. 55, no. 14, pp. 14–21, 2022, 11th IFAC Symposium on Intelligent Autonomous Vehicles IAV 2022.

[14] M. Malekzadeh, D. Manolis, I. Papamichail, and M. Papageorgiou, "Empirical investigation of properties of lane-free automated vehicle traffic," in *2022 IEEE 25th International Conference on Intelligent Transportation Systems (ITSC)*. IEEE, 2022, pp. 2393–2400.

[15] P. Kincaid, "The rule of the road: an international guide to history and practice," 1986.

[16] M. Rostami-Shahrbabaki, H. Zhang, M. Sekeran, and K. Bogenberger, "Increasing the capacity of a lane-free beltway for connected and automated vehicles using potential lines," in *102nd Annual Meeting Transportation Research Board*, 2023.

[17] M. M. Zefreh and A. Török, "Distribution of traffic speed in different traffic conditions: An empirical study in budapest," *Transport*, vol. 35, no. 1, pp. 68–86, 2020.

[18] M. S. Bains, B. Ponnu, and S. S. Arkatkar, "Modeling of traffic flow on indian expressways using simulation technique," *Procedia-Social and Behavioral Sciences*, vol. 43, pp. 475–493, 2012.

[19] J. E. Angus, "The probability integral transform and related results," *SIAM Review*, vol. 36, no. 4, pp. 652–654, 1994.

[20] J. L. Catbagan and H. Nakamura, "Desired speed distributions on two-lane highways under various conditions," *Transportation Research Record*, vol. 2088, no. 1, pp. 218–226, 2008. [Online]. Available: https://doi.org/10.3141/2088-23

[21] D. Troullinos, G. Chalkiadakis, D. Manolis, I. Papamichail, and M. Papageorgiou, "Lane-free microscopic simulation for connected and automated vehicles," in *2021 IEEE International Intelligent Transportation Systems Conference (ITSC)*, 2021, pp. 3292–3299.

[22] M. Behrisch, L. Bieker, J. Erdmann, and D. Krajzewicz, "Sumo–simulation of urban mobility: An overview," in *Proceedings of SIMUL 2011, The Third International Conference on Advances in System Simulation*. ThinkMind, 2011.

[23] D. Troullinos, G. Chalkiadakis, D. Manolis, I. Papamichail, and M. Papageorgiou, "Extending sumo for lane-free microscopic simulation of connected and automated vehicles," in *SUMO Conference Proceedings*, vol. 3, 2022, pp. 95–103.